FUZZY LOGIC BASED A BIDIRECTIONAL DC/DC CONVERTER WITH DUAL-BATTERY ENERGY STORAGE FOR HYBRID ELECTRIC VEHICLE SYSTEM

[1]G. SAI SURAJ **(M.TECH)** ,[2] Mr. R.ANIL KUMAR**M.TECH (Assistant Professor)** ,

[3] Mr. P.PRASANTH KUMAR **M.TECH (Assistant Professor)**

GOKARAJU RANGARAJU INSTITUTE OF ENGINEERING AND TECHNOLOGY, TELANGANA,INDIA.

ABSTRACT

This paper proposes a modern multi-input dc–dc converter with fuzzy control based on a hybrid energy system. We use a fuzzy controller in this paper because it has certain advantages over other controllers. The fuzzy controller is best for human decision-making because it combines the function of an automated device with expert decisions.The proposed converter can be used to transfer energy between various sources of energy. Battery charging mode and battery discharging mode are the two modes of operation for the proposed converter.Power is delivered to the output from all input sources. By allowing active power sharing, the proposed converter is used to regulate the power of ESSs. The used ESSs' voltage levels can be higher or lower than the output voltage.The use of a fuzzy controller for a nonlinear system reduces uncertain effects in system control while also increasing performance. We will study the novel bidirectional non-isolated multi-input converter (MIC) topology for hybrid systems to be used in electric vehicles using the simulation results.

Index Terms*—Bidirectional dc/dc converter (BDC), dual battery storage, hybrid electric vehicle*.

I. INTRODUCTION

Bi-directional dc-dc converters have recently been extensively researched and developed for a wide range of applications, including battery chargers and dischargers, electric cars, and UPS systems.In case of the battery fed electric vehicles (BFEVs), electric energy flows between motor and battery side. For achieving zero emission, the vehicle can be powered only by batteries or other electrical energy sources. Batteries have widely been adopted in ground vehicles due to their characteristics in terms of high energy density, compact size, and reliability. This can be applied in Hybrid Electric Vehicle (HEVs) with a battery as an energy storage element to provide desired management of the power flows. In hybrid electric vehicle energy storage devices act as catalysts to provide energy boost. However the high initial cost of BFEVs as well as its short driving range has limited its use. Bidirectional dc-dc converters are the key components of the traction systems in Hybrid Electric Vehicles. The use of a Bi-directional dc-dc converter fed dc motor drive devoted to electric vehicles (EVs) application allows a suitable control of both motoring and regenerative braking operations, and it can contribute to a significant increase the drive system overall efficiency.

Figure 1 shows a practical diagram for a standard (FCV/HEV) power system [4, 13]. Furthermore, ES1 is used as the main battery storage system for supplying peak power, while ES2 is used as an auxiliary battery storage device to achieve the vehicle range extender principle [13]. The aim of a bidirectional dc/dc converter (BDC) is to link dual-battery energy storage to the driving inverter's dc-bus.

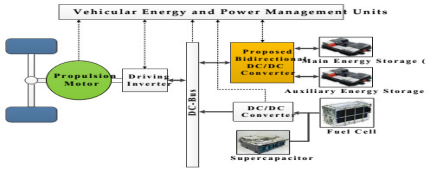

Fig. 1. Typical functional diagram for a FCV/HEV power system

Several multiport BDCs have been designed to provide unique voltages for loads while also controlling power flow between various sources, lowering overall cost, mass, and power consumption.

Isolated and non-isolated BDCs are two different forms of BDCs.

II. Bidirectional power flow topology

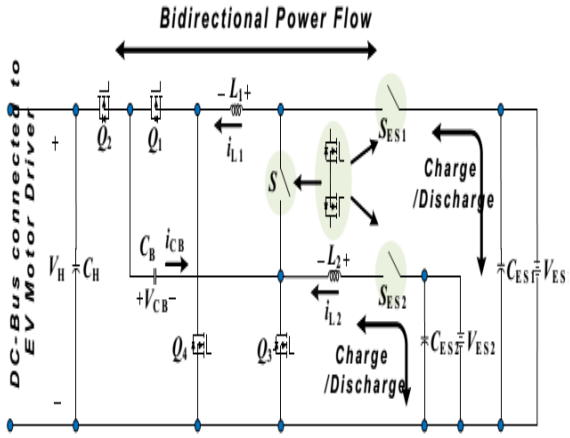

Fig.2.Proposed BDC topology with dual-battery energy storage

In Fig. 2, the proposed BDC topology with dual-battery energy storage is shown, where VH, VES1, and VES2 reflect the system's high-voltage dc-bus voltage, main energy storage (ES1), and auxiliary energy storage (ES2) respectively. Two bidirectionalIn the converter structure, power switches (SES1 and SES2) are used to turn on and off the current loops of ES1 and ES2, respectively.To increase the static voltage gain between the two low-voltage dual sources (VES1, VES2) and the high-voltage dc bus (VH), a charge-pump capacitor (CB) is integrated as a voltage divider with four active switches (Q1, Q2, Q3, Q4) and two phase inductors (L1, L2). Furthermore, the additional CB reduces the switch voltage stress of active switches and eliminates the need to operate at an extreme duty ratio.Furthermore, the three bidirectional power switches (S, SES1, SES2) shown in Fig. 2 are used to regulate the power flow between two low-voltage dual sources (VES1, VES2) and to block either positive or negative voltage. Two metal-oxide-semiconductor field-effect transistors (MOSFETs) pointing in opposite directions are connected in series to create this bidirectional power transferTable I displays all of the conduction statuses of the power devices involved in each operation mode to demonstrate the idea for the proposed converter. As a result, to aid comprehension, the four operating modes are depicted as follows.

TABLE I.
CONDUCTION STATUS OF DEVICES FOR DIFFERENT OPERATING MODES

Operating Modes	ON	OFF	Control Switch	Synchronous Rectifier (SR)
Low-voltage dual-source-powering mode (Accelerating, x_1=1, x_2=1)	S_{ES1}, S_{ES2}	S	Q_3, Q_4	Q_1, Q_2
High-voltage dc-bus energy-regenerating mode (Braking, x_1=1, x_2=1)	S_{ES1}, S_{ES2}	S	Q_1, Q_2	Q_3, Q_4
Low-voltage dual-source buck mode (ES1 to ES2, x_1=0, x_2=0)	S_{ES1}, S_{ES2}	Q_1, Q_2, Q_4	S	Q_3
Low-voltage dual-source boost mode (ES2 to ES1, x_1=0, x_2=0)	S_{ES1}, S_{ES2}	Q_1, Q_2, Q_4	Q_3	S
System shutdown	-	S_{ES1}, S_{ES2} Q_1, Q_2, Q_3, Q_4	-	-

In addition, either positive or negative voltage can be blocked. Two metal-oxide-semiconductor field-effect transistors (MOSFETs) pointing in opposite directions are connected in series to create this bidirectional power transfer.

III .A. Low-Voltage Dual-Source-Powering Mode

The circuit schematic and steady-state waveforms for the converter in low-voltage dual-source-powering mode are shown in Fig. 3(a). The switch S is switched off, the switches (SES1, SES2) are turned on, and the two low-voltage dual sources (VES1, VES2) provide power to the dc-bus and loads. The low-side switches Q3 and Q4 are actively switching at a phase-shift modeangle of 180° , and the high-side switches Q1 and Q2 function as the synchronous rectifier (SR).

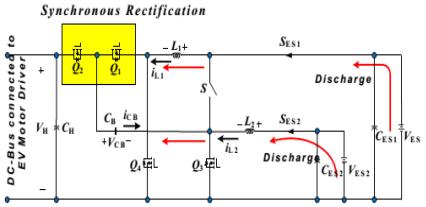

Fig 3(a):Low-voltage dual-source-powering mode of BDC

a).State 1 [t0 < t < t1]: The interval time is (1-Du)Tsw, switches Q1, Q3 are on, and switches Q2, Q4 are off in this state. The difference between the low-side voltage VES1 and the charge-pump voltage (VCB) is the voltage around L1, and thus iL1 decreases linearly from its initial value. In addition, the energy source VES2 charges the inductor L2.,

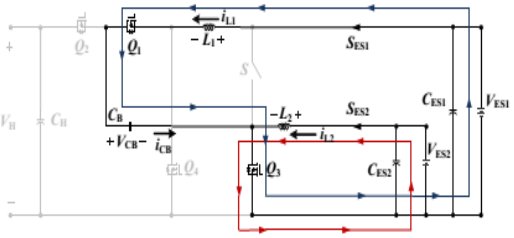

(a)

b) State 2 [t1 < t < t2]: The interval time is (Du-0.5)Tsw in this state, and switches Q3 and Q4 are on while switches Q1 and Q2 are off. Low-side voltages raise inductor currents, causing energy to flow into storage.

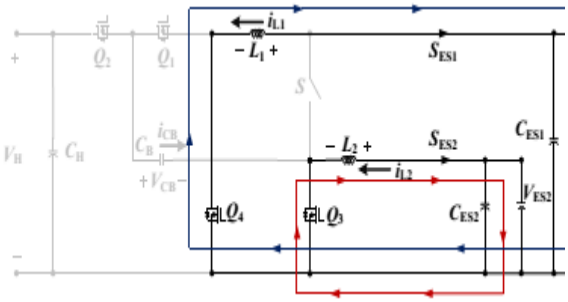

(b)

c) State 3 [t2 < t < t3]: The interval time is (1-Du)Tsw in this state, and switches Q1 and Q3 are on, while switches Q2 and Q4 are off.

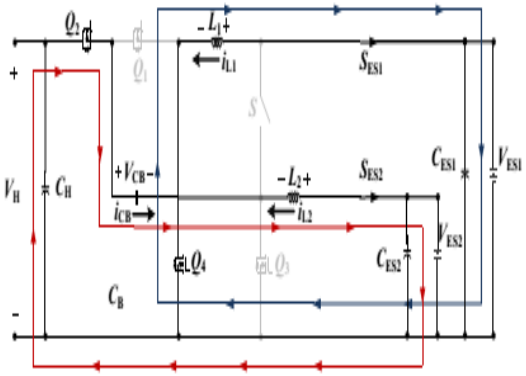

(c)

d) State 4 [t3 < t < t4]: The interval time is (0.5-Dd)Tsw in this state, and switches Q3 and Q4 are on, while switches Q1 and Q2 are off.

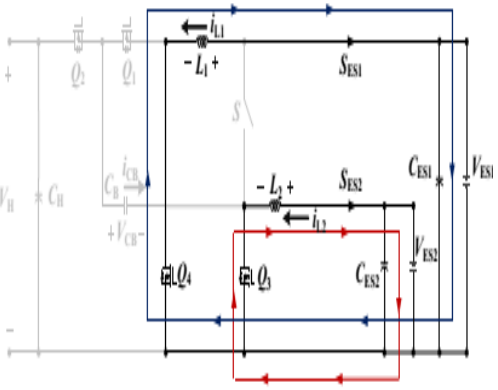

(d)

Fig. 3(b). Circuit states of the proposed BDC for the Low voltage dual Source powering mode. (a) State 1. (b) State 2. (c) State 3. (d) State 4.

B. High-Voltage DC-Bus Energy-Regenerating Mode

During regenerative braking, the kinetic energy stored in the motor drive is fed back to the source in this mode. The regenerative capacity can be significantly increased. In this state, the interval time is (Du-0.5)Tsw, and switches Q3 and Q4 are turned on while switches Q1 and Q2

are turned off.Low-side voltages cause energy to flow into storage by increasing inductor currents. greater than the battery's capacity to consume As a result, the extra energy is put to good use by charging the energy storage unit. Under the high-voltage dc bus energy-regenerating mode, the circuit schematic and steady-state waveforms of the BDC are shown.

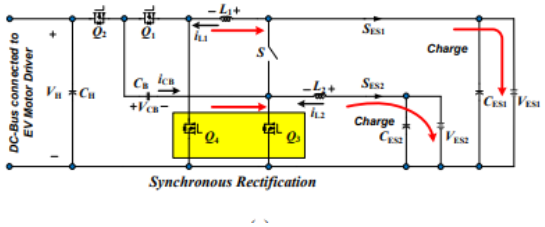

Fig4. Schematic diagram for High-Voltage DC-Bus Energy-Regenerating Mode

a) State 1 [t0 < t < t1]: The interval time is (1-Du)Tsw, switches Q1, Q3 are on, and switches Q2, Q4 are off in this state. The difference between the low-side voltage VES1 and the charge-pump voltage (VCB) is the voltage around L1, and thus iL1 decreases linearly from its initial value. In addition, the energy source VES2 charges the inductor L2.,

$$L_1 \frac{di_{L1}}{dt} = V_{ES1} - V_{CB}$$

$$L_2 \frac{di_{L2}}{dt} = V_{ES2}$$

b) State 2 [t1 < t < t2]: The interval time is (0.5-Dd) Tsw in this state, and switches Q3 and Q4 are on, while switches Q1 and Q2 are off. Since the voltages across inductors L1 and L2 are positive in comparison to the low-side voltages VES1 and VES2, inductor currents iL1 and iL2 increase linearly. These voltages are denoted by the letters

$$L_1 \frac{di_{L1}}{dt} = V_{ES1}$$

$$L_2 \frac{di_{L2}}{dt} = V_{ES2}$$

c) State 3 [t2 < t < t3]: The interval time is Dd Tsw in this state, and switches Q1 and Q3 are switched off, while switches Q2 and Q4 are turned on. The positive low-side voltage VES1 is applied across L1, so iL1 increases linearly from its initial value. The voltage through L2 is also negative since it is the difference between the high-side voltage VH, the charge-pump voltage VCB, and the low-side voltage VES2.

$$L_1 \frac{di_{L1}}{dt} = V_{ES1}$$

$$L_2 \frac{di_{L2}}{dt} = V_{CB} + V_{ES2} - V_H$$

d) State 4 [t3 < t < t4]: The interval time is (0.5-Dd)Tsw in this state, and switches Q3 and Q4 are on, while switches Q1 and Q2 are off. The voltages around the inductors L1 and L2 are written as

$$L_1 \frac{di_{L1}}{dt} = V_{ES1}$$

$$L_2 \frac{di_{L2}}{dt} = V_{ES2}$$

C. Low-Voltage Dual-Source Buck/Boost Mode

Figure 5 shows the circuit schematic for this mode, which includes transferring energy from the main

energy storage to the auxiliary energy storage and vice versa. The topology is then converted to a single-leg bidirectional buck-boost converter in this section.

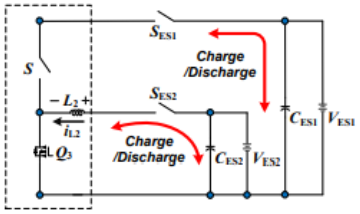

Fig. 5. Low-voltage dual-source buck/boost mode of the proposed BDC

The buck converter channels power from main energy storage to auxiliary energy storage when the duty cycle of the active bidirectional switch S is regulated, as shown in Fig. 6. Power flows from the auxiliary energy storage to the main energy storage when the duty cycle of switch Q3 is operated, indicating that the converter is operating in boost mode, as shown in Fig.7.

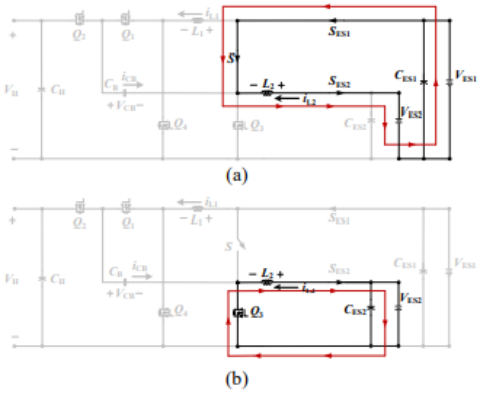

Fig. 6. Circuit states of the proposed BDC for the low-voltage dual-source buck mode. (a) State 1. (b) State 2.

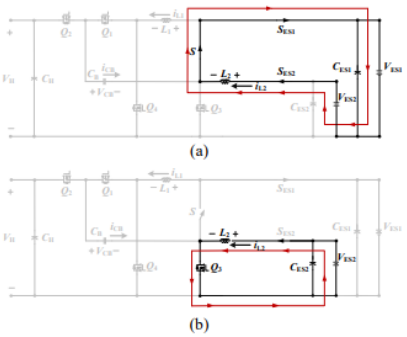

Fig. 7. Circuit states of the proposed BDC for the low-voltage dual-source boost mode. (a) State 1. (b) State 2

IV.CONVERTER CONTROL

The converter control structure is depicted in Fig. 8(a), which includes a vehicular strategic management stage and the proposed BDC controller. For comparison, Fig. 8(b) shows the operating modes of the proposed BDC.

Electrical power demand estimation is part of the strategic management level, which also includes a vehicular power and voltage management unit. The management's overall results must optimise the use of the source that best fits power demand while still meeting the needs of the drivers and routes[21,25-33].The dc-bus voltage of the converter in FCV/HEV power systems (Fig. 1) is depicted in Fig. 8(a), which includes a vehicular strategic management stage and the proposed BDC controller. operating modes of the proposed BDC is shown in Fig. 8(b). As a result, rather than regulating the converter output voltage in each operation mode, the inductor current iL1 or iL2 is detected and compared to the reference current to regulate the power flow, as shown in Fig. 8. (a).

The vehicular energy, power, and voltage management unit selects the BDC mode in the converter control structure based on the operating conditions of the vehicle, such as power demand of different driving states (Pdem) and dual-source voltages (VES1, VES2).). The Fuzzy logic controller then selects the necessary current references iL1ref or iL2ref to guide the active switches (S, Q1Q4). The service cycle dictated by different switch selector statuses is converted into gate control signals for the power switches using the pulsed-width-modulation (PWM) switching scheme.

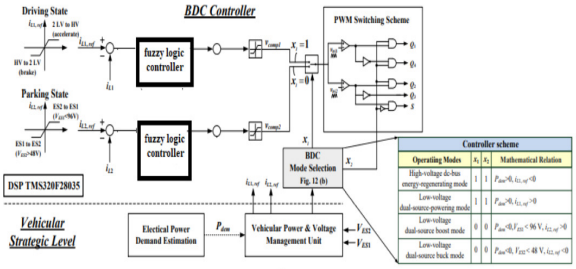

Fig. 8. (a) Block diagram of the closed-loop control scheme

The current reference iL1,ref is used to monitor bidirectional power flow between the low-voltage dual-source and the high-voltage dc-bus, as shown in Fig. 8(a) (i.e., 2 LV to HV or HV to 2 LV). Because of the proposed BDC topology's inherent uniform average current sharing, the average inductor current iL2 is equal to the regulated average inductor current iL1.The current reference iL2,ref, on the other hand, is used to monitor the power flow between the main and auxiliary energy storage (i.e., ES1 to ES2 or ES2 to ES1).

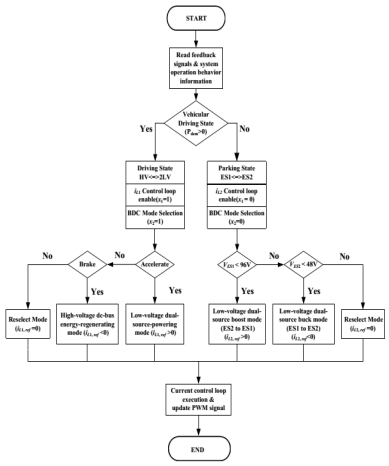

(b)

8 (b) flowchart for various operating modes of the proposed BD C.

The mode switching method is shown in Fig. 8(b) and is depicted above . To begin, when the vehicle is in the driving mode (Pdem>0), the controller is in the iL1 control loop (x1=1), and the vehicle is either accelerating (iL1,ref>0, HV to 2 LV) or braking (iL1,ref 0, 2 LV to HV). If none of these conditions exists, it will execute reselect mode to process the next mode switching decision..In addition, when the vehicle is in the parking state (Pdem0), the controller is in the iL2 control loop (x1=0). In this state, mode switching decision is based on the voltages of VES1 (96 V) and VES2 (96 V) (48 V). The mode is low-voltage dual-source boost mode (iL2,ref>0, VES2 to VES1) . the mode is low-voltage dual-source buck mode (iL2,ref<0, VES1 to VES2). If both situations do not be satisfied, it executes reselect mode to process the next.

V. FUZZY LOGIC CONTROLLER

Fuzzy logic control mostly consists of three stages: a)Fuzzification b) Rule base c) Defuzzification During fuzzification, numerical input variables are

converted into linguistic variable based on a membership functions. For these MPP techniques the inputs to fuzzy logic controller are taken as a change in power w.r.t change in current E and change in voltage error C. Once E and Care calculated and converted to the linguistic variables, the fuzzy controller output, which is the duty cycle ratio D of the power converter, can be search for rule base table. The variables assigned to D for the different combinations of E and C is based on the intelligence of the user.

Why Should We Use Fuzzy Controllers?

- It is very robust
- It can be easily modified
- It can use multiple inputs and outputs sources
- Much simpler than its predecessors (linear algebraic equations)

Architecture of Fuzzy Logic Controller :

The architecture of the fuzzy logic controller shown in Fig. 9 includes four components: Fuzzifier, Rule Base, Fuzzy Inference Engine (decision making unit), and Defuzzifier.

Fuzzifier: Fuzzy logic uses linguistic variables instead of numerical variables. In a control system, error between reference signal and output signal can be assigned as Negative Big (NB), Negative Medium (NM), Negative Small (NS), Zero (ZE), Positive small (PS), Positive Medium (PM), Positive Big (PB). The triangular membership function is used for fuzzifications.

The process of fuzzification convert numerical variable (real number) to a linguistic variable (fuzzy number) so that it can be matched with the premises of the fuzzy rules defined in the application specific rule base.

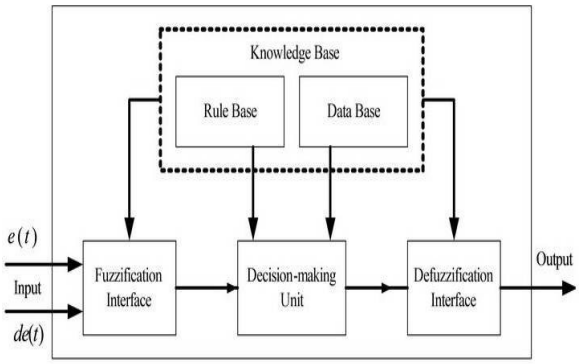

Fig. 9 Architecture of Fuzzy Logic Controller

Rule Base:

E CE	NB	NM	NS	Z	PS	PM	PB
PB	Z	PS	PM	PB	PB	PB	PB
PM	NS	Z	PS	PM	PB	PB	PB
PS	NM	NS	Z	PS	PM	PB	PB
Z	NB	NM	NS	Z	PS	PM	PB

The rule base includes a set of fuzzy if-then rules that describe the controller's behaviour in terms of linguistic variables and linguistic term membership functions. The linguistic control rules required by the rule evaluator are stored in the Rule base (decision making logic). The fuzzy controller's output is an estimate of the magnitude of peak reference current.This peak comparison current includes the non-linear load's active power demand as well as distribution system losses. The desired reference current is calculated by multiplying the peak reference current by the PLL output. Catalogue: The specification of the triangular membership feature required by fuzzifier and defuzzifier is stored in the Database.

Fuzzy Inference Engine: The fuzzy inference engine generates a fuzzy output set by applying the inference function to the set of rules in the fuzzy rule base. This entails matching the input fuzzy set with the rules' premises, activating the rules to deduce each rule's conclusion, and combining all enabled conclusions using fuzzy set union to produce fuzzy set production.

Defuzzifier: The rules of fuzzy logic controller generate required output in a linguistic variable (Fuzzy Number), according to real world requirements; linguistic variables have to be transformed to crisp output (Real number). This selection of strategy is a compromise between accuracy and computational intensity.

Fig10. Simulink model of fuzzy system:

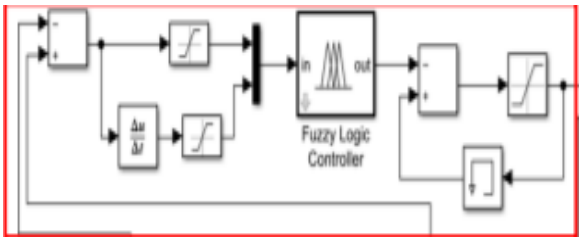

Table. 2 The Membership Functions For FLC

The three stages of fuzzy logic are (a) fuzzification, (b) inference, and (c) defuzzification. A membership is used to transform data into fuzzified inputs based on the input. In addition, to arrive at conclusions, a rule-based inference process is framed. To produce control feedback to the method, these conclusions must go through a defuzzification phase. The system of fuzzy logic approach has the drawback that the defuzzification process takes significant time and memory.

VI. SIMULATION RESULTS

The results of simulations were used to confirm the proposed model's accuracy.

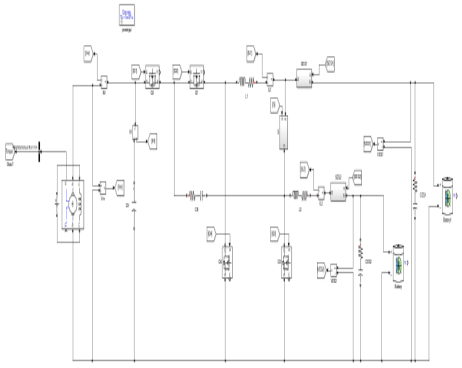

Fig11 Simulink model of proposed system

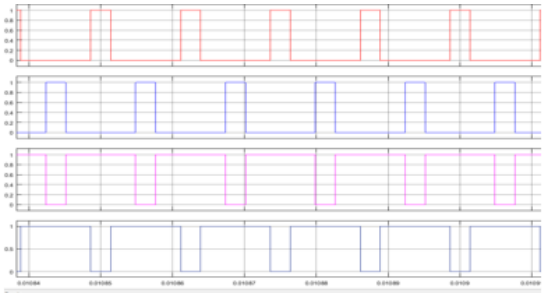

12(a)

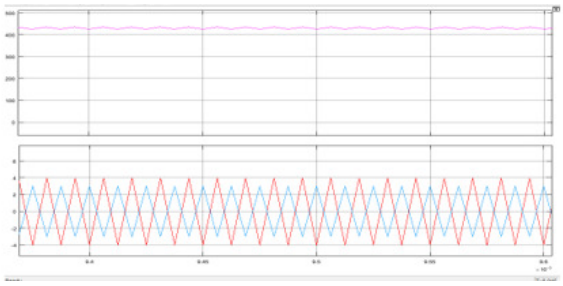

Fig. 12 waveforms for low-voltage dual-source-powering mode: (a) gate signals; (b) outputvoltage and inductor currents.

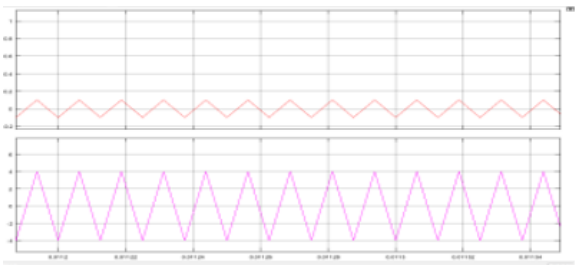

13(a)

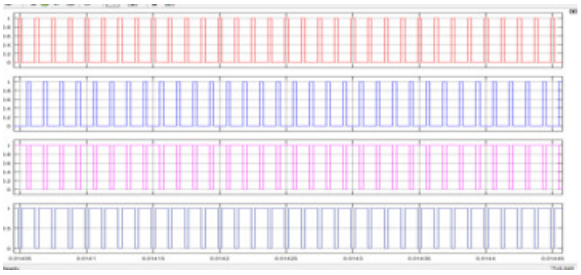

Fig. 13.waveforms for high -voltage dual-source-powering mode: (a) gate signals; (b) output voltage and inductor currents.

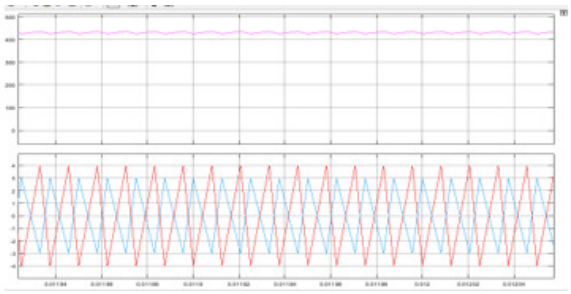

14(a)

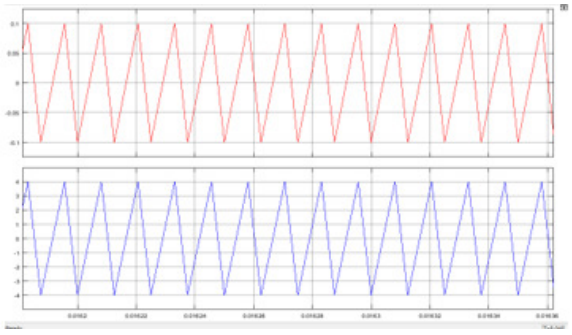

fig 14 . Waveforms of controlled current step change in the low-voltage dual-source-powering mode: (a) by simulation; and (b)*iH*is changed from 0 to 0.85 A; *iL*1 is changed from 0 tox 2.5 A; Time/Div=20 ms/Div)

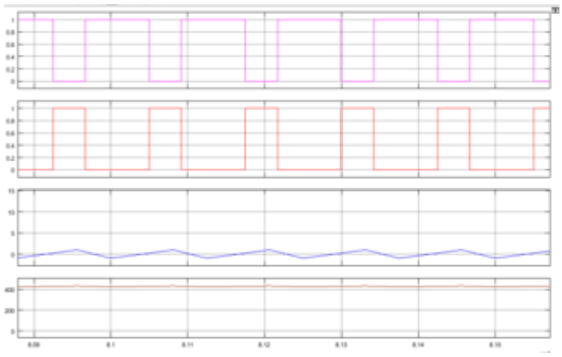

15(a)

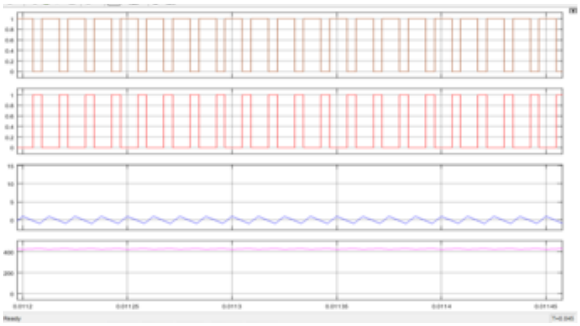

Fig.15. waveforms of gate signals, output voltage and inductor currents for the low-voltage dual-source buck/boost mode: (a) buck mode; (b) boost mode.

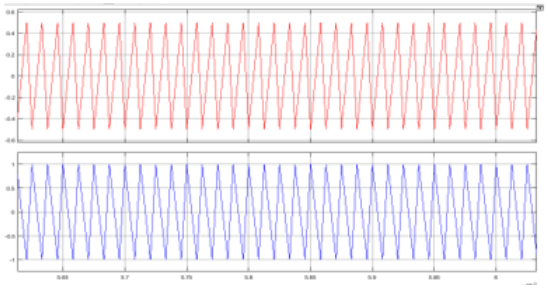

Fig16(a)

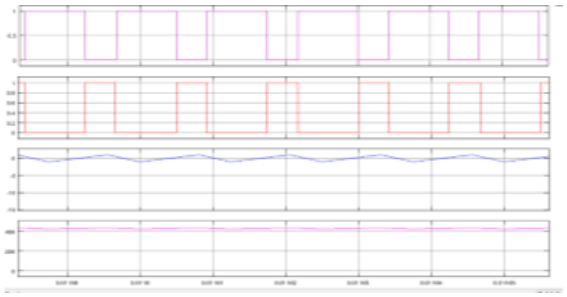

Fig.16(b). Waveforms of controlled current step change in the high-voltage dc-bus energy-regenerating mode: (a) by simulation of voltage (b)current

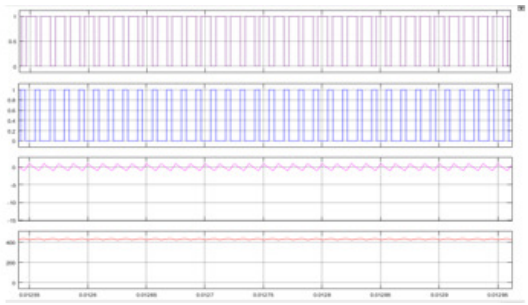

17(a)

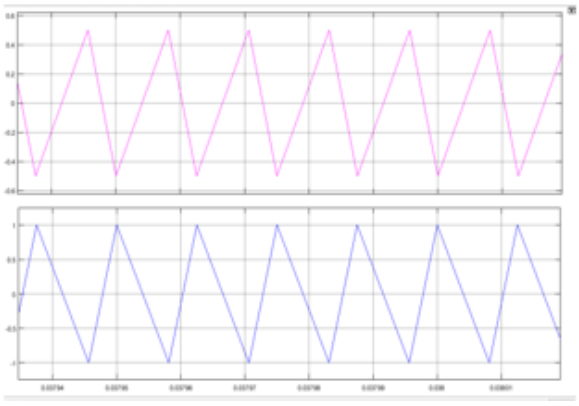

Fig17(b) Waveforms of controlled current step change in the low-voltage dual- source buck mode: (a) by simulation of voltage and (b) current

CONCLUSIONS

To interface dual battery energy sources and high-voltage dc buses of various voltage levels, a new BDC topology was presented. The circuit configuration, principles of operation, and analyses and the proposed BDC's static voltage gains were addressed on the foundation of various power transfer modes.The fuzzy controller increases battery life by smoothing the current and reducing settling time and peak overshoot of the DC connection voltage. A bidirectional buck-boost converter is used by the fuzzy logic controller to regulate the battery's power flow. In MATLAB/SIMUINK, the entire energy management system has been tested with various modes of operation such as low voltage dualsource powering mode, high voltage regenerating mode, boost/buck modes.

REFERENCES

[1] M. Ehsani, K. M. Rahman, and H. A. Toliyat, "Propulsion system design of electric and hybrid vehicles," IEEE Transactions on industrial electronics, vol. 44, no. 1, pp. 19-27, 1997.

[2] A. Emadi, K. Rajashekara, S. S. Williamson, and S. M. Lukic, "Topological overview of hybrid electric and fuel cell vehicular power system architectures and configurations," IEEE Transactions on Vehicular Technology, vol. 54, no. 3, pp. 763-770, 2005. [3] A. Emadi, S. S. Williamson, and A. Khaligh, "Power electronics intensive solutions for advanced electric, hybrid electric, and fuel cell vehicular power systems," IEEE Transactions on Power Electronics, vol. 21, no. 3, pp. 567-577, 2006.

[4] E. Schaltz, A. Khaligh, and P. O. Rasmussen, "Influence of battery/ultracapacitor energy-storage sizing on battery lifetime in a fuel cell hybrid electric vehicle," IEEE Transactions on Vehicular Technology, vol. 58, no. 8, pp. 3882-3891, 2009.

[5] P. Thounthong, V. Chunkag, P. Sethakul, B. Davat, and M. Hinaje, "Comparative study of fuel-cell vehicle hybridization with battery or supercapacitor storage device," IEEE transactions on vehicular technology, vol. 58, no. 8, pp. 3892-3904, 2009.

[6] C. C. Chan, A. Bouscayrol, and K. Chen, "Electric, hybrid, and fuel-cell vehicles: Architectures

and modeling," IEEE transactions on vehicular technology, vol. 59, no. 2, pp. 589-598, 2010.

[7] A. Khaligh and Z. Li, "Battery, ultracapacitor, fuel cell, and hybrid energy storage systems for electric, hybrid electric, fuel cell, and plug-in hybrid electric vehicles: State of the art," IEEE transactions on Vehicular Technology, vol. 59, no. 6, pp. 2806-2814, 2010.

[8] K. Rajashekara, "Present status and future trends in electric vehicle propulsion technologies," IEEE Journal of Emerging and Selected Topics in Power Electronics, vol. 1, no. 1, pp. 3-10, 2013.

[9] C.-M. Lai, Y.-C. Lin, and D. Lee, "Study and implementation of a two-phase interleaved bidirectional DC/DC converter for vehicle and dc-microgrid systems," Energies, vol. 8, no. 9, pp. 9969-9991, 2015.

[10] C.-M. Lai, "Development of a novel bidirectional DC/DC converter topology with high voltage conversion ratio for electric vehicles and DC-microgrids," Energies, vol. 9, no. 6, p. 410, 2016.

[11] J. Moreno, M. E. Ortúzar, and J. W. Dixon, "Energy-management system for a hybrid electric vehicle, using ultracapacitors and neural networks," IEEE transactions on Industrial Electronics, vol. 53, no. 2, pp. 614-623, 2006.

[12] J. Bauman and M. Kazerani, "A comparative study of fuel-cell–battery, fuel-cell–ultracapacitor, and fuel-cell–battery–ultracapacitor vehicles," IEEE Transactions on Vehicular Technology, vol. 57, no. 2, pp. 760-769, 2008.

[13] M. Ehsani, Y. Gao, and A. Emadi, Modern electric, hybrid electric, and fuel cell vehicles: fundamentals, theory, and design . CRC press, 2009.

[14] Z. Haihua and A. M. Khambadkone, "Hybrid modulation for dual active bridge bi-directional converter with extended power range for ultracapacitor application," in Industry Applications Society Annual Meeting, 2008. IAS'08. IEEE, 2008, pp. 1-8: IEEE.

[15] H. Tao, J. L. Duarte, and M. A. Hendrix, "Three-port triple-half-bridge bidirectional converter with zero-voltage switching," IEEE transactions on power electronics, vol. 23, no. 2, pp. 782-792, 2008.

[16] T. Bhattacharya, V. S. Giri, K. Mathew, and L. Umanand, "Multiphase bidirectional flyback converter topology for hybrid electric vehicles," IEEE Transactions on Industrial Electronics, vol. 56, no. 1, pp. 78-84, 2009.

[17] H. Krishnaswami and N. Mohan, "Three-port series-resonant DC–DC converter to interface renewable energy sources with bidirectional load and energy storage ports," IEEE Transactions on Power Electronics, vol. 24, no. 10, pp. 2289-2297, 2009.

[18] Y.-C. Liu and Y.-M. Chen, "A systematic approach to synthesizing multi-input DC–DC converters," IEEE Transactions on Power Electronics, vol. 24, no. 1, pp. 116-127, 2009.

[19] K. Gummi and M. Ferdowsi, "Double-input dc–dc power electronic converters for electric-drive vehicles—Topology exploration and synthesis using a single-pole triple-throw switch," IEEE Transactions on Industrial Electronics, vol. 57, no. 2, pp. 617-623, 2010.

[20] B. Zhao, Q. Song, and W. Liu, "Power characterization of isolated bidirectional dual-active-bridge DC–DC converter with dual-phase-shift control," IEEE Transactions on Power Electronics, vol. 27, no. 9, pp. 4172-4176, 2012.

[21] L. Jiang, C. C. Mi, S. Li, M. Zhang, X. Zhang, and C. Yin, "A novel soft-switching bidirectional DC–DC converter with coupled inductors," IEEE Transactions on Industry Applications, vol. 49, no. 6, pp. 2730-2740, 2013.

[22] D.-Y. Jung, S.-H. Hwang, Y.-H. Ji, J.-H. Lee, Y.-C. Jung, and C.-Y. Won, "Soft-switching bidirectional DC/DC converter with a LC series resonant circuit," IEEE Transactions on Power Electronics, vol. 28, no. 4, pp. 1680-1690, 2013.

[23] H. Wu, K. Sun, S. Ding, and Y. Xing, "Topology derivation of nonisolated three-port DC–DC converters from DIC and DOC," IEEE Transactions on Power Electronics, vol. 28, no. 7, pp. 3297-3307, 2013.

[24] B. Farhangi and H. A. Toliyat, "Modeling and analyzing multiport isolation transformer capacitive components for onboard vehicular power conditioners," IEEE Transactions on Industrial Electronics, vol. 62, no. 5, pp. 3134-3142, 2015.

[25] A. Hintz, U. R. Prasanna, and K. Rajashekara, "Novel modular multiple-input bidirectional DC–DC power converter (MIPC) for HEV/FCV application," IEEE Transactions on Industrial Electronics, vol. 62, no. 5, pp. 3163-3172, 2015.

[26] A. Nahavandi, M. T. Hagh, M. B. B. Sharifian, and S. Danyali, "A nonisolatedmultiinput multioutput DC–DC boost converter for electric vehicle applications," IEEE Transactions On Power Electronics, vol. 30, no. 4, pp. 1818-1835, 2015.

[27] C.-M. Lai and M.-J. Yang, "A high-gain three-port power converter with fuel cell, battery sources and stacked output for hybrid electric vehicles and DC-microgrids," Energies, vol. 9, no. 3, p. 180, 2016.

[28] Y. Jang and M. M. Jovanovic, "Interleaved boost converter with intrinsic voltage-doubler characteristic for universal-line PFC front end," IEEE Transactions on Power Electronics, vol. 22, no. 4, pp. 1394-1401, 2007.

[29] C.-M. Lai, Y.-J. Lin, M.-H. Hsieh, and J.-T. Li, "A newly-designed multiport bidirectional power converter with battery/supercapacitor for hybrid electric/fuel-cell vehicle system," in Transportation Electrification Asia-Pacific (ITEC Asia-Pacific), 2016 IEEE Conference and Expo, 2016, pp. 163-166: IEEE.

[30] R. de Castro, R. E. Araujo, J. P. F. Trovao, P. G. Pereirinha, P. Melo, and D. Freitas, "Robust DC-link control in EVs with multiple energy storage systems," IEEE Transactions on Vehicular Technology, vol. 61, no. 8, pp. 3553-3565, 2012.